

Vibrational Analysis of Peptides, Polypeptides, and Proteins. XV. Crystalline Polyglycine II

A. M. DWIVEDI and S. KRIMM, *Biophysics Research Division, The University of Michigan, Ann Arbor, Michigan 48109*

Synopsis

A force field has been refined for the 3_1 -helix structure of polyglycine II, using the polyglycine I force field plus previous $C^\alpha H^\alpha \cdots O$ force constants as a starting point. Besides force constants associated with the hydrogen bonds, which must change since the hydrogen-bond characteristics are different in the two structures, we have had to modify only 10 force constants from the polyglycine I force field to make it suitable for reproducing the polyglycine II frequencies. Most involve the NC^α bond, which is the torsion angle that changes from the I to the II structure. Calculations were done for parallel chain and antiparallel chain crystal structures of polyglycine II, the observed spectra being found to agree best with the latter structure. Since this provides strong evidence for the loss of strict threefold symmetry in the chain, our analysis strengthens the support for the existence of $C^\alpha H^\alpha \cdots O$ hydrogen bonds in the structure of polyglycine II.

INTRODUCTION

Early powder x-ray studies¹ of the structure of polyglycine II [(Gly)_nII] led to the proposal that the polypeptide chain is a 3_1 -helix. Subsequent work has supported this conclusion, and thus this molecule serves as a useful model for polypeptides with a threefold helical backbone symmetry. It is therefore important that all aspects of its structure and spectrum be understood in detail.

The originally proposed crystal structure¹ consisted of a hexagonal array of parallel chains hydrogen-bonded to each other via $N-H \cdots O=C$ bonds, although it was noted that the lattice could accommodate an inverted chain. In a small modification of the original structure, it was suggested² that the $C=O$ group could also participate in $C^\alpha-H^\alpha \cdots O=C$ hydrogen bonds. Subsequent ir studies^{3,4} provided experimental support for the presence of such bonds. On the basis of mechanical transformation of (Gly)_nII to (Gly)_nI, as well as morphological considerations, it was pointed out⁵ that (Gly)_nII must contain antiparallel chains, and a specific crystal structure was subsequently proposed for such an arrangement.⁶

Normal mode analyses of (Gly)_nII to date⁷⁻¹⁰ have been based on the isolated chain. This is not completely satisfactory, since even with explicit inclusion of the CH_2 group,¹⁰ these calculations cannot predict a fairly large number of observed frequencies and splittings.^{4,8,11-13}

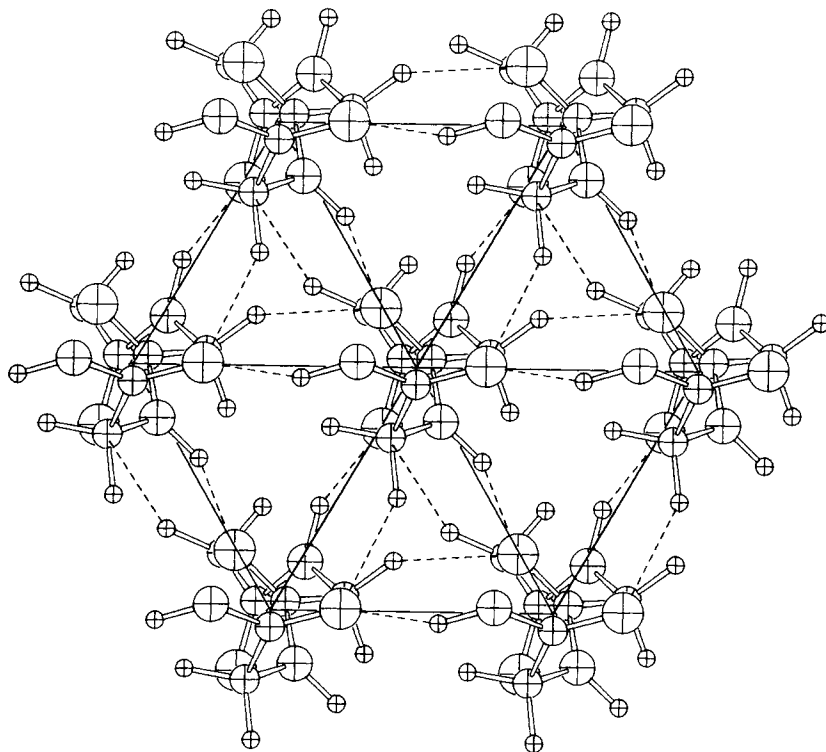


Fig. 1. Parallel chain structure of polyglycine II.

We have calculated the normal modes of crystalline $(\text{Gly})_n\text{II}$, for both parallel and antiparallel structures, and we are able to predict and assign most of the frequencies that are not accounted for by the single-chain calculations. Our results also indicate that the antiparallel chain arrangement is the more likely one in the crystal.

NORMAL-MODE CALCULATION

Structure, Symmetry, and Selection Rules

The single-chain geometry that we used is based on the same bond lengths and angles as were used for $(\text{Gly})_n\text{I}$.^{14,15} The backbone is a 3_1 -helix with an axial repeat of $c = 9.30 \text{ \AA}$, which corresponds to dihedral angles of $\varphi = -76.89^\circ$ and $\psi = 145.32^\circ$.

The parallel chain crystal structure² is based on a hexagonal cell with $a = 4.80 \text{ \AA}$; a c -axis projection with up-directed chains is shown in Fig. 1. The antiparallel chain crystal structure may be variable,⁶ but for purposes of the normal-mode calculation, it can be satisfactorily represented by an

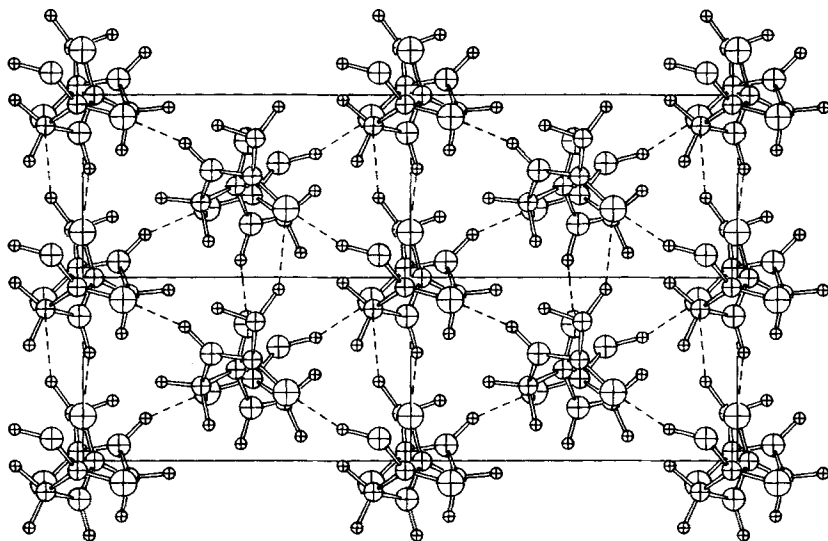
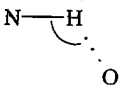
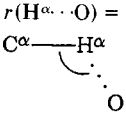
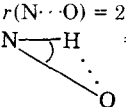
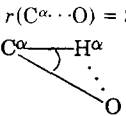
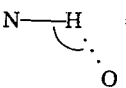
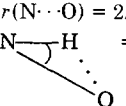


Fig. 2. Antiparallel chain structure of polyglycine II.

orthorhombic cell with two oppositely directed chains.⁶ This unit cell, having $a = 8.487 \text{ \AA}$ and $b = 4.80 \text{ \AA}$, is shown in Fig. 2, and it has the chains related by a twofold screw axis at $a/4$ and perpendicular to the ac plane. In order to have optimum hydrogen bonds and other intermolecular contacts, the chains are arranged as follows.^{2,6} The chains are first fixed with α -carbon atoms located on the lines connecting the lattice of helix axes. Each chain is then rotated 10° about the helix axis from this position. For the parallel chain structure, all the chains are rotated counterclockwise as viewed in Fig. 1. For the antiparallel chain structure, the up-chains have a counterclockwise rotation of 10° , while the down-chains have a clockwise rotation of the same amount. In both cases, all $\text{N}-\text{H} \cdots \text{O}=\text{C}$ hydrogen bonds can be formed, although their characteristics are slightly different (see Table I for details). In the parallel chain arrangement, all CH_2 groups can participate in $\text{C}^\alpha-\text{H}^\alpha \cdots \text{O}=\text{C}$ bonds; in the antiparallel chain arrangement, however, only a third of the CH_2 groups are involved in such interactions (the parameters of these bonds are also given in Table I). It should be noted that $\text{C}^\alpha-\text{H}^\alpha \cdots \text{O}=\text{C}$ bonds in the antiparallel chain structure are made only between like-directed chains. As we will see, the loss of strict threefold chain symmetry in the latter case has important consequences with respect to the spectrum of this structure.

For the parallel chain structure there is one chain per unit cell, and since the three residues are equivalent, the smallest unit for purposes of the calculation is a single chemical residue of the chain. The unit cell has C_3 symmetry, and the optically active symmetry coordinates are therefore classified into A and E species, given by¹⁰

TABLE I
 Interchain Hydrogen Bonds in Crystalline Polyglycine II

Parallel Chain Structure ^a	
$r(\text{H} \cdots \text{O}) = 1.729 \text{ \AA}$  $r(\text{H}^{\alpha} \cdots \text{O}) = 2.360 \text{ \AA}$ 	$r(\text{N} \cdots \text{O}) = 2.683 \text{ \AA}$  $r(\text{C}^{\alpha} \cdots \text{O}) = 3.327 \text{ \AA}$ 
Antiparallel Chain Structure ^a	
$r(\text{H} \cdots \text{O}) = 1.748 \text{ \AA}$ 	$r(\text{N} \cdots \text{O}) = 2.693 \text{ \AA}$ 

^a Interchain bond distances and angles correspond to chain bond lengths and angles given in Ref. 14.

$$S(\text{A}) = C \sum_i (S_{\text{I}}^i + S_{\text{II}}^i + S_{\text{III}}^i)$$

$$S^c(\text{E}) = C' \sum_i (2S_{\text{I}}^i - S_{\text{II}}^i - S_{\text{III}}^i)$$

$$S^s(\text{E}) = C'' \sum_i (S_{\text{II}}^i - S_{\text{III}}^i)$$

where S_{I}^i , S_{II}^i , and S_{III}^i are local symmetry coordinates of the three chemical residues of the chain in the i th unit cell, and C , C' , and C'' are normalization constants. $S^c(\text{E})$ and $S^s(\text{E})$ are a pair of real symmetry coordinates for the degenerate E species, corresponding to phase differences of $\pm 2\pi/3$, respectively, between adjacent residues. (The A species corresponds to a phase difference of zero.) There are 20 A-species modes and 20 E-species modes, all ir and Raman active.

For the antiparallel chain structure, since each chain no longer has strict threefold symmetry, the smallest unit for purposes of calculation consists of the three residues in the structural repeat of a single chain. The unit cell has C_2 symmetry, and the optically active symmetry coordinates are classified into A and B species, given by

$$S(\text{A}) = C' \sum_i (S_{\text{I}}^i + S_{\text{II}}^i)$$

$$S(\text{B}) = C'' \sum_i (S_{\text{I}}^i - S_{\text{II}}^i)$$

where S_{I}^i and S_{II}^i are the local symmetry coordinates of chains I and II of the i th unit cell, and C' and C'' are normalization constants. Of the total

of 123 normal modes, 62 are A and 61 are B species. All of these are both ir and Raman active.

The local symmetry coordinates used in this calculation are the same as those used previously.¹⁵ In addition, we required coordinates for the $C^\alpha-H^\alpha \cdots O=C$ interaction. These were taken to be $H^\alpha \cdots O$ stretch, $C^\alpha H^\alpha \cdots O$ in-plane bend, and $CO \cdots H^\alpha$ in-plane bend, and were applicable to all CH_2 groups of the parallel chain structure and every appropriate third CH_2 group of the antiparallel chain structure.

Force Field

The starting point for the refinement of the $(Gly)_n$ II force field was the recently revised force field for $(Gly)_n$ I,¹⁵ plus the $C^\alpha H^\alpha \cdots O$ constants used in an earlier simplified calculation.³ Frequencies were obtained for both parallel chain and antiparallel chain structures, and when it became clear that the latter were favored by the data, the refinement was concentrated on this structure. The final list of force constants is given in Table II. Subsequent calculations for the parallel chain structure then made use of the appropriate subset of these force constants.

As noted above, in the antiparallel chain structure, every third residue in a chain is involved in a $C^\alpha-H^\alpha \cdots O=C$ hydrogen bond. It is therefore necessary to allow for peptide-group force constants that are associated with bifurcated hydrogen bonds, as well as those associated with typical $N-H \cdots O=C$ hydrogen bonds. Neither of these kinds of force constants will be expected to have values identical to those in $(Gly)_n$ I, since the hydrogen bonds in the two structures have different strengths. The $C^\alpha-H^\alpha \cdots O=C$ hydrogen bond, of course, introduces force constants not present in $(Gly)_n$ I [just as the $H^\alpha \cdots H^\alpha$ interaction in $(Gly)_n$ I is absent in $(Gly)_n$ II]. With respect to the remaining intramolecular force field, we have tried to transfer without change as many force constants as possible, making adjustments only where required by the spectral data. Ten such changes were needed, which is a surprisingly small number in view of the significant conformational difference between a β -sheet chain and a 3_1 -helical chain. [For $(Gly)_n$ I, $\varphi = 149.9^\circ$ and $\psi = 146.5^\circ$, compared to $\varphi = -76.9^\circ$ and $\psi = 145.3^\circ$ for $(Gly)_n$ II.] We present below some of the considerations involved in guiding our choice of various force constants.

The existence of two kinds of NH groups (involving typical and bifurcated hydrogen bonds) should be detectable through the presence of two NH stretching bands in the spectrum. Although the ir spectrum^{4,11} shows only one band, near 3303 cm^{-1} , the Raman spectrum⁸ definitely exhibits two amide A modes, at 3305 cm^{-1} (weak) and 3278 cm^{-1} (medium). These have relative frequencies and intensities consistent with an assignment to a bifurcated and a typical hydrogen bond, respectively. In order to obtain the unperturbed frequencies, it is necessary to do a Fermi resonance analysis.¹⁴ For this, we have taken amide B, at 3086 cm^{-1} ,^{8,11} to be the same for both amide A bands (since no splitting is observed in this band),

TABLE II
 Force Constants for Crystalline Polyglycine II

Force Constant ^a	Value ^b	Force Constant ^a	Value ^b
1. $f(\text{NC}^\alpha)^{*c}$	4.843	27. $f(\text{NH} \cdots \text{O ib})_b^\ddagger$	0.050
2. $f(\text{C}^\alpha\text{C})$	4.409	28. $f(\text{CO} \cdots \text{H}^\alpha \text{ ib})^\ddagger$	0.020
3. $f(\text{CN})$	6.415	29. $f(\text{C}^\alpha\text{H}^\alpha \cdots \text{O ib})^\ddagger$	0.020
4. $f(\text{CO})^*$	9.621	30. $f(\text{CO ob})^*$	0.487
5. $f(\text{NH})^*$	5.720	31. $f(\text{CO ob})_b^\ddagger$	0.537
6. $f(\text{NH})_b^\ddagger$ ^d	5.856	32. $f(\text{NH ob})$	0.129
7. $f(\text{C}^\alpha\text{H})$	4.564	33. $f(\text{NC}^\alpha\text{t})$	0.037
$f(\text{C}^\alpha\text{H}^\alpha)$		34. $f(\text{C}^\alpha\text{Ct})$	0.037
8. $f(\text{C}^\alpha\text{H})_b^\ddagger$	4.780	35. $f(\text{CN t})$	0.680
9. $f(\text{C}^\alpha\text{H}^\alpha)_b^\ddagger$	4.430	36. $f(\text{NH t})^*$	0.0035
10. $f(\text{H} \cdots \text{O})^*$	0.160	37. $f(\text{CO t})$	0.001
11. $f(\text{H} \cdots \text{O})_b^\ddagger$	0.110	38. $f(\text{NC}^\alpha, \text{C}^\alpha\text{C})$	0.300
12. $f(\text{H}^\alpha \cdots \text{O})^{\text{te}}$	0.050	39. $f(\text{C}^\alpha\text{C}, \text{CN})$	0.300
13. $f(\text{NC}^\alpha\text{C})^*$	1.150	40. $f(\text{NC}^\alpha, \text{CN})$	0.300
14. $f(\text{C}^\alpha\text{CN})^*$	1.300	41. $f(\text{C}^\alpha\text{C}, \text{CO})$	0.500
15. $f(\text{CNC}^\alpha)^*$	0.487	42. $f(\text{CN}, \text{CO})$	0.500
16. $f(\text{NCO})^*$	1.166	43. $f(\text{C}^\alpha\text{H}^\alpha, \text{C}^\alpha\text{H})^*$	-0.015
17. $f(\text{NC}^\alpha\text{H})$	0.715	44. $f(\text{C}^\alpha\text{H}^\alpha, \text{C}^\alpha\text{H})_b^\ddagger$	-0.050
$f(\text{NC}^\alpha\text{H}^\alpha)$		45. $f(\text{C}^\alpha\text{H}^\alpha, \text{H}^\alpha \cdots \text{O})^\ddagger$	0.080
18. $f(\text{NC}^\alpha\text{H})_b$	0.715	46. $f(\text{NC}^\alpha, \text{CNC}^\alpha)$	0.300
19. $f(\text{NC}^\alpha\text{H}^\alpha)_b^\ddagger$	0.785	47. $f(\text{NC}^\alpha, \text{NC}^\alpha\text{C})$	0.300
20. $f(\text{C}^\alpha\text{NH})^*$	0.537	48. $f(\text{NC}^\alpha, \text{C}^\alpha\text{NH})$	0.294
$f(\text{C}^\alpha\text{NH})_b^\ddagger$	0.532	49. $f(\text{NC}^\alpha, \text{NC}^\alpha\text{H})$	0.517
21. $f(\text{C}^\alpha\text{CO})$	1.166	$f(\text{NC}^\alpha, \text{NC}^\alpha\text{H}^\alpha)$	
22. $f(\text{CC}^\alpha\text{H})$	0.684	50. $f(\text{NC}^\alpha, \text{CC}^\alpha\text{H})$	0.026
$f(\text{CC}^\alpha\text{H}^\alpha)$		$f(\text{NC}^\alpha, \text{CC}^\alpha\text{H}^\alpha)$	
$f(\text{CC}^\alpha\text{H})_b$		51. $f(\text{C}^\alpha\text{C}, \text{NC}^\alpha\text{C})$	0.300
$f(\text{CC}^\alpha\text{H}^\alpha)_b$		52. $f(\text{C}^\alpha\text{C}, \text{C}^\alpha\text{CN})$	0.300
23. $f(\text{CNH})^*$	0.537	53. $f(\text{C}^\alpha\text{C}, \text{C}^\alpha\text{CO})$	0.200
$f(\text{CNH})_b^\ddagger$	0.532	54. $f(\text{C}^\alpha\text{C}, \text{NC}^\alpha\text{H})$	0.026
24. $f(\text{H}^\alpha\text{C}^\alpha\text{H})^*$	0.560	$f(\text{C}^\alpha\text{C}, \text{NC}^\alpha\text{H}^\alpha)$	
25. $f(\text{CO} \cdots \text{H ib})$	0.010	55. $f(\text{C}^\alpha\text{C}, \text{CC}^\alpha\text{H})$	0.205
26. $f(\text{NH} \cdots \text{O ib})^*$	0.057	$f(\text{C}^\alpha\text{C}, \text{CC}^\alpha\text{H}^\alpha)$	

(continued)

and we have assumed that the observed ir band contains an overlap of both amide A modes. Using an overall area intensity ratio $I_B/I_A = 0.125$,⁴ and assuming that this is equally applicable to the two modes, we find for the above amide A bands that $\nu_A^\circ = 3279 \text{ cm}^{-1}$, $\nu_B^\circ = 3110 \text{ cm}^{-1}$ and $\nu_A^\circ \approx 3257 \text{ cm}^{-1}$, $\nu_B^\circ = 3108 \text{ cm}^{-1}$, respectively. (It is interesting that the overtone of the observed amide II band at 1554 cm^{-1} is 3108 cm^{-1} , suggesting that resonance occurs between such overtones and each of the two NH fundamentals.) The lower ν_A° frequency is significantly below that for (Gly)_nI, viz., 3272 cm^{-1} ,¹⁵ which is reasonable in terms of the much shorter hydrogen bond in (Gly)_nII [$r(\text{N} \cdots \text{O}) = 2.69 \text{ \AA}$] than in (Gly)_nI [$r(\text{N} \cdots \text{O}) = 2.91 \text{ \AA}$]. Similarly, the higher frequency ν_A° value suggests that the bifurcated bond is slightly weaker than that in (Gly)_nI.

TABLE II (continued)

Force Constant ^a	Value ^b	Force Constant ^a	Value ^b
56. $f(\text{CN}, \text{C}^\alpha\text{CN})$	0.300	72. $f(\text{NC}^\alpha\text{H}^\alpha, \text{NH ob})$	0.1022
57. $f(\text{CN}, \text{CNC}^\alpha)$	0.300	73. $f(\text{NC}^\alpha\text{H}, \text{NH ob})$	0.0456
58. $f(\text{CN}, \text{NCO})$	0.200	74. $f(\text{C}^\alpha\text{CO}, \text{CC}^\alpha\text{H}^\alpha)$	0.150
59. $f(\text{CN}, \text{CNH})$	0.294	75. $f(\text{C}^\alpha\text{CO}, \text{CC}^\alpha\text{H})$	0.100
60. $f(\text{CO}, \text{C}^\alpha\text{CO})$	0.450	76. $f(\text{NCO}, \text{CNH})$	0.251
61. $f(\text{CO}, \text{NCO})$	0.450	77. $f(\text{C}^\alpha\text{NH}, \text{CNH})$	0.0065
62. $f(\text{CO}, \text{C}^\alpha\text{CN})$	-0.150	78. $f(\text{C}^\alpha\text{NH}, \text{NC}^\alpha\text{H}^\alpha)^*$	0.051
63. $f(\text{NC}^\alpha\text{C}, \text{C}^\alpha\text{NH})$	-0.100	79. $f(\text{C}^\alpha\text{NH}, \text{NC}^\alpha\text{H})^*$	0.061
64. $f(\text{NC}^\alpha\text{C}, \text{NC}^\alpha\text{H})$ } $f(\text{NC}^\alpha\text{C}, \text{NC}^\alpha\text{H}^\alpha)$ }	-0.031	80. $f(\text{CC}^\alpha\text{H}, \text{CC}^\alpha\text{H}^\alpha)$	-0.032
65. $f(\text{NC}^\alpha\text{C}, \text{CO}, \text{ob})$	-0.0725	81. $f(\text{CC}^\alpha\text{H}, \text{HC}^\alpha\text{H}^\alpha)$ } $f(\text{CC}^\alpha\text{H}^\alpha, \text{HC}^\alpha\text{H}^\alpha)$ }	0.0398
66. $f(\text{NC}^\alpha\text{C}, \text{NH ob})$	0.1092	82. $f(\text{CC}^\alpha\text{H}, \text{CO ob})$ } $f(\text{CC}^\alpha\text{H}^\alpha, \text{CO ob})$ }	0.100
67. $f(\text{C}^\alpha\text{CN}, \text{CNH})$	0.200	83. $f(\text{CO ob}, \text{NH ob})$	0.010
68. $f(\text{CNC}^\alpha, \text{C}^\alpha\text{NH})$	-0.040	84. $f(\text{NH} \cdot \cdot \text{O ib}, \text{NH ob})^*$	-0.005
69. $f(\text{CNC}^\alpha, \text{NC}^\alpha\text{H})^*$	0.270	85. $f(\text{CO ob}, \text{CN t})$	0.0111
70. $f(\text{NC}^\alpha\text{H}, \text{CC}^\alpha\text{H})$ } $f(\text{NC}^\alpha\text{H}^\alpha, \text{CC}^\alpha\text{H}^\alpha)$ }	0.019	86. $f(\text{NH ob}, \text{CN t})$	-0.1677
71. $f(\text{NC}^\alpha\text{H}, \text{HC}^\alpha\text{H}^\alpha)$ } $f(\text{NC}^\alpha\text{H}^\alpha, \text{HC}^\alpha\text{H}^\alpha)$ }	0.0615		

^a $f(\text{AB}) = \text{AB}$ bond stretch, $f(\text{ABC}) = \text{ABC}$ angle bend, $f(\text{X}, \text{Y}) = \text{XY}$ interaction; ib = in-plane bend, ob = out-of-plane bend, t = torsion.

^b Units are $\text{mdyn}/\text{\AA}$ for stretch and stretch, stretch force constants, mdyn for stretch, bend force constants, and $\text{mdyn}/\text{\AA}$ for all others.

^c Asterisk denotes force constants whose values in polyglycine II are different from those in polyglycine I (cf. Ref. 15).

^d Subscript b denotes force constants applicable to bifurcated hydrogen bond.

^e Dagger denotes new force constants applicable to polyglycine II.

The values of $f(\text{NH})$ and $f(\text{NH})_b$ depend on the choice of $f(\text{H} \cdot \cdot \text{O})$ and $f(\text{H} \cdot \cdot \text{O})_b$ (the subscript b designates the group involved in the bifurcated bond). Since *a priori* knowledge of force constants for hydrogen bonds is still very limited, we were guided in these choices by our experience with other polypeptide systems. For $f(\text{H} \cdot \cdot \text{O})$, we selected a value, $0.160 \text{ mdyn}/\text{\AA}$, slightly higher than that for β -poly(L-alanine), viz., $0.150 \text{ mdyn}/\text{\AA}$,¹⁶ and consistent with the variation in this force constant with $r(\text{N} \cdot \cdot \text{O})$ from β - (2.73 \AA) to α -poly(L-alanine) (data to be published) (2.86 \AA). For $f(\text{H} \cdot \cdot \text{O})_b$, we chose a smaller value, since this bond is expected to be weaker,¹⁷ and then set $f(\text{H}^\alpha \cdot \cdot \text{O})$ so that the sum of these was 0.160 . This was influenced by the determination that the observed amide I splitting could be accounted for completely by transition dipole coupling^{18,19} using the same value of $f(\text{C}=\text{O})$ for all three groups in the helix repeat, and therefore the hydrogen-bonding effect on $\text{C}=\text{O}$ should be about the same whether it participates in a typical or in a bifurcated bond. Although the choices are slightly arbitrary, they are certainly reasonable ones at this stage. Changes in other force constants associated with the $\text{N}-\text{H} \cdot \cdot \text{O}=\text{C}$ hydrogen bond, namely, $f(\text{NH} \cdot \cdot \text{O ib})$, $f(\text{CO ob})$, $f(\text{NH t})$, and

TABLE III
Observed and Calculated Frequencies (in cm^{-1}) of Crystalline Polyglycine II

Raman	Observed ^a IR	Calculated				Potential Energy Distribution ^b
		Antiparallel		Parallel		
		A	B	A	E	
3279W ^c	3279S ^c	3281	3281	3281	3281	NH s(98)
3257M ^c		3254	3254			NH s(97)
2979S	2977W	2980	2980	2981	2980	NH s(97)
2940VS	2935MW	2936	2936			CH ₂ as(78), CH ₂ ss(18)
		2936	2936			CH ₂ as(99)
	2850MW	2853	2853			CH ₂ ss(99)
	2805W	2803	2803	2803	2804	CH ₂ ss(82), CH ₂ as(22)
1654VS	~1655W	1656	1654	1658		CO s(71), CN s(20), C ^α CN d(10)
		1651	1653			CO s(74), CN s(20), C ^α CN d(10)
1560W	1640VS	1649	1645		1649	CO s(72), CN s(20), C ^α CN d(10)
	~1560W	1565	1565			CO s(73), CN s(19), C ^α CN d(10)
	1550S	1555	1552			CO s(73), CN s(20), C ^α CN d(10)
		1548	1548			CO s(74), CN s(19), C ^α CN d(10)
	1432W	1433	1433	1533		NH ib(59), CN s(18)
		1422	1423	1435	1431	NH ib(56), CN s(20), C ^α C s(10)
1421S	1420M	1421	1421			NH ib(51), CN s(21), C ^α C s(13)
1388MS	1377M	1383	1380	1374		NH ib(54), CN s(21), C ^α C s(12)
						NH ib(55), CN s(18), C ^α C s(12)
						CH ₂ b(90)
						CH ₂ b(80)
						CH ₂ b(82)
						CH ₂ b(79)
						CH ₂ w(58), C ^α C s(15), NH ib(13)
						CH ₂ w(58), NH ib(18), C ^α C s(13)
						CH ₂ w(68), NH ib(12), C ^α C s(11)

1334VW	~1332VW	1350	1350	CH ₂ w(46), CH ₂ b(16), NH ib(16), C ^α C s(14)
		1344	1345	CH ₂ w(50), NH ib(16), CH ₂ b(14), C ^α C s(13)
1283M	1283M	1303	1304	CH ₂ tw(31), NH ib(14), CH ₂ w(13), CN s(12)
1261S		1290	1290	CH ₂ tw(36), NH ib(22)
			1274	CH ₂ tw(29), CH ₂ w(23), NH ib(13), CN s(12)
		1266	1267	CH ₂ tw(89)
		1249	1249	CH ₂ tw(86)
1244MS				CH ₂ tw(47), CH ₂ w(17), CN s(13)
1134M	1132W	1237	1237	CH ₂ tw(53), CH ₂ w(13), CN s(11)
		1131	1131	CH ₂ w(28), CN s(25), NC ^α s(22), NH ib(18)
1031VS	1028M	1039	1038	CH ₂ tw(67)
		1037	1038	CH ₂ w(29), CH ₂ tw(23), CN s(17), NC ^α s(18), NH ib(10)
		974	1038	NC ^α s(58), C ^α C s(14)
968VW	971VW	970	975	NC ^α s(70), C ^α C s(11)
		965	969	CH ₂ r(63), C ^α C s(10)
952W		961		CH ₂ r(69)
		958		CH ₂ r(59), C ^α C s(12)
897VW	901M	902		CH ₂ r(61), C ^α C s(10)
		889		CH ₂ r(66)
884VS		872	885	C ^α C s(19), CH ₂ r(17), CN s(17), CO s(12)
864W	862VW	871	871	C ^α C s(18), CH ₂ r(18), CN s(18), CO s(12)
		760	762	CH ₂ r(26), C ^α C s(16), CN s(16), CO s(10)
752VW	751W	740		CH ₂ r(21), CN s(18), C ^α C s(17), CO s(11)
742VW				CH ₂ r(23), C ^α C s(21), NC ^α C d(12), CN s(12)
				CH ₂ r(33), C ^α C s(19), NC ^α C d(12), CN s(11)
				NH ob(17), NC ^α C d(15), CO ib(14), CNC ^α d(10), CN s(10)
				CN t(20), NH ob(19), NH...O ib(14), NC ^α C d(13), CO ib(12)
				CN t(53), NH...O ib(22), NH ob(18)

(continued)

TABLE III (continued)

Raman	Observed ^a IR	Calculated			Potential Energy Distribution ^b
		Antiparallel A	B	Parallel A E	
	740M		738		CN t(49), NH··O ib(20), NH ob(16), CO ib(11) CN t(68), NH ob(31), NH··O ib(30) CN t(69), NH··O ib(23), NH ob(17), CO ib(11) CO ib(28), NC ^α C d(18) CO ib(25), NC ^α C d(17), CN t(11), CO ob(10)
707W			714	716	729
	698S	{ 711 710	710		713
673M		{ 674 664	678		CO ib(26), NC ^α C d(18) CO ib(27), NC ^α C d(18) CN t(77), NH ob(27), NH t(11), CO ob(10) CN t(83), NH ob(28), NH t(11), NH··O ib(10) CN t(88), NH ob(30), NH t(14) CO ob(64) CO ob(60), CO ib(14), C ^α C s(10) CO ob(59), CO ib(11), NH ob(10) CO ob(59), CO ib(11) CO ob(61), NH ob(13) CO ob(59), NH ob(13) CO ob(60), NH ob(13) CO ob(59), NH ob(15), CN t(10) C ^α CN d(38), CO ib(12), NC ^α s(12)
578W		{ 584	581	588	589
566M	573S		569		
		{ 566 563	562		
496W		{ 498 496	498		501
353VW	363S		494		
340M		{ 355	352		353
313VW		{ 348	349		
272W	267M		324	328	
		{ 270	270	276	
					NH ob(21), CO ob(21) NH ob(22), CO ob(22) NH ob(23), CO ob(21), CNC ^α d(10), NC ^α s(10)

237	237	237	CNC ^α d(60), CO ib(13), H··O s(12)
		228	CNC ^α d(35), H··O s(24), C ^α CN d(20)
			CNC ^α d(66), CO ib(12)
			CNC ^α d(72), CO ib(12)
		194	CNC ^α d(55), C ^α CN d(21)
217W	221		C ^α CN d(45), CNC ^α d(22), NC ^α s(12)
203W	193		H··O s(34), CN t(23)
	133		CN t(31), H ^α ··O s(30), NH ob(14), NH··O ib(11)
		130	CN t(29), CNC ^α d(17), NH··O ib(15), H ^α ··O s(15)
			CN t(30), NH··O ib(16), H··O s(10)
		120	CN t(38), NH ob(19), H··O s(13), NH··O ib(11)
		116	CN t(39), NH··O ib(12), NH ob(10), H ^α ··O s(10)
113M	116		H··O s(28), NH ob(17), CN t(17), CO t(14), NH t(11), C ^α C t(11)
	97		NH ob(35), CO t(18), NC ^α t(14), NC ^α d(13), CN t(10)
		94	NH ob(24), NC ^α d(16), H ^α ··O s(12), NC ^α t(11)
		85	NH ob(43), NH··O ib(20), H··O s(11), NH t(11), CO··H ib(10)
83W	85		NH ob(35), NH t(23), C ^α H ^α ··O ib(19)
		78	NH ob(41), NC ^α d(16), C ^α C t(14), NH··O ib(12), H··O s(11)
		74	NH ob(49), NC ^α d(20), C ^α C t(15)
		73	NH ob(45), C ^α C t(18), NC ^α d(17), NH··O ib(10)
	72		NH ob(38), NH··O ib(31), CN t(13), NH t(10)
	67		C ^α C t(24), NH ob(18)
~50VW	50	63	NH ob(31), H··O s(12), NC ^α d(11), C ^α H ^α ··O ib(10), CO t(10)
		43	NH ob(34), H··O s(20), NH··O ib(16), CO··H ib(11)
	29		NH t(41), CO t(16), NH ob(12), CO··H ib(11)

^a VS = very strong, S = strong, M = medium, W = weak, VW = very weak.

^b s = stretch, as = antisymmetric stretch, ss = symmetric stretch, b = angle bend, ib = in-plane angle bend, ob = out-of-plane angle bend, w = wag, r = rock, t = torsion, d = deformation, tw = twist. Only contributions of 10% or greater are included. In some cases where contributions to the PEDs of related A and B modes differ by less than 3% the average value has been given for both frequencies.

^c Unperturbed frequency (see text).

$f(\text{NH} \cdots \text{O ib}, \text{NH ob})$, are not surprising, nor is the necessity of introducing additional force constants associated with the $\text{C}^\alpha\text{—H}^\alpha \cdots \text{O}=\text{C}$ hydrogen bond, namely, $f(\text{CO} \cdots \text{H}^\alpha \text{ ib})$, $f(\text{C}^\alpha\text{H}^\alpha \cdots \text{O ib})$, and $(\text{C}^\alpha\text{H}^\alpha, \text{H}^\alpha \cdots \text{O})$.

With respect to the force constants for the CH_2 group, different values are obviously required for the nonbonded and bonded groups. For the former, using the assignments proposed previously,³ we found that $f(\text{C}^\alpha\text{H})$ and $f(\text{C}^\alpha\text{H}^\alpha)$ could be kept the same as in $(\text{Gly})_n\text{I}$, but $f(\text{H}^\alpha\text{C}^\alpha\text{H})$ had to be reduced slightly. This is reasonable because of the absence of the $\text{H}^\alpha \cdots \text{H}^\alpha$ interaction of $(\text{Gly})_n\text{I}$. In addition, the larger separation between the antisymmetric and symmetric CH_2 stretch frequencies in $(\text{Gly})_n\text{II}$ has necessitated a change in sign for $f(\text{C}^\alpha\text{H}^\alpha, \text{C}^\alpha\text{H})$. For the bonded CH_2 group, we have, as before,³ made the bonded force constant, $f(\text{C}^\alpha\text{H}^\alpha)_b$, lower than the nonbonded, $f(\text{C}^\alpha\text{H})_b$, and allowed $f(\text{C}^\alpha\text{H}^\alpha, \text{C}^\alpha\text{H})$ to adjust to the observed separation of CH_2 stretch frequencies. It is also possible that the change in $f(\text{NC}^\alpha\text{H}^\alpha)_b$ is associated with this hydrogen bond, as is the absence of $f(\text{NC}^\alpha\text{H}, \text{NC}^\alpha\text{H}^\alpha)$.

Of about 70 intramolecular force constants in $(\text{Gly})_n\text{I}$ that do not involve the hydrogen bonds directly, only 10 have required adjustment, and of these the largest percentage changes occur in 7 force constants associated with the N—C^α bond. This is undoubtedly significant, since the φ dihedral angle undergoes a large change between $(\text{Gly})_n\text{I}$ and $(\text{Gly})_n\text{II}$, while the ψ angle is essentially the same. The 10 force constants that change, with their $(\text{Gly})_n\text{I}$ and $(\text{Gly})_n\text{II}$ values, are $f(\text{NC}^\alpha)$: 5.043, 4.843; $f(\text{NC}^\alpha\text{C})$: 0.819, 1.150; $f(\text{C}^\alpha\text{CN})$: 1.400, 1.300; $f(\text{CNC}^\alpha)$: 0.687, 0.487; $f(\text{NCO}) = f(\text{C}^\alpha\text{CO})$: 1.246, 1.166; $f(\text{CNC}^\alpha, \text{NC}^\alpha\text{H})$: 0.000, 0.270; $f(\text{C}^\alpha\text{NH}, \text{NC}^\alpha\text{H}^\alpha)$: 0.100, 0.051; $f(\text{C}^\alpha\text{NH}, \text{NC}^\alpha\text{H})$: 0.031, 0.061; $f(\text{NC}^\alpha\text{H}, \text{NC}^\alpha\text{H}^\alpha)$: 0.0463, 0.000. This shows that while the force field is substantially independent of conformation, there definitely are some conformation-dependent force constants. This has already been seen for β -poly(L-alanine)^{12,16} as compared to α -poly(L-alanine) (data to be published and Ref. 21) and is an important subject for further detailed elucidation.

RESULTS AND DISCUSSION

The calculated frequencies for $(\text{Gly})_n\text{II}$ in the antiparallel chain and parallel chain structures are given in Table III and compared with observed Raman and ir data.^{3,4,8,11,13} In Table IV we present the calculated frequencies for the N-deuterated molecule, $(\text{Gly})_n\text{II-ND}$, in the antiparallel chain structure and compare these with published Raman⁸ and ir¹¹ results.

Most of the assignments are similar to those of Abe and Krimm,¹⁰ although because their calculation was for a single chain without explicit hydrogen bonds, some assignments and particularly potential-energy distributions differ. In addition, we calculate many more frequencies, which are, in fact, observed. This is particularly evident on comparing the results for the antiparallel chain and parallel chain structures given in Table

III and is the main reason for suggesting that $(\text{Gly})_n$ II adopts the former structure. It should be noted that this difference in the number of bands is not a result of the presence of two chains in the unit cell of the former as compared to only one in the latter; as can be seen from Table III, crystal splittings are very small. Rather, the difference arises from the fact that in the parallel chain structure all three residues in the repeat of a single chain are equivalent (all having bifurcated hydrogen bonds), thus giving rise to A- and E-species helical chain modes. In the case of the antiparallel chain structure the three residues are not equivalent (only one participates in a bifurcated hydrogen bond), and this loss of strict threefold symmetry in a single chain gives rise to significant intrachain frequency splittings. The larger number of observed bands than expected for an exact 3_1 -helical structure is a strong qualitative argument for the loss of threefold symmetry and, therefore, for the presence of $\text{C}^\alpha\text{—H}^\alpha \cdots \text{O}=\text{C}$ hydrogen bonds in only some of the residues, as is predicted for the antiparallel chain structure.^{2,6} We discuss the various assignments in greater detail below.

Polyglycine II

The NH stretch modes have already been considered. We only note here that each frequency is localized in a single NH bond in the repeating unit of three residues, with the 3281-cm^{-1} mode being associated with the bifurcated bond.

The four observed CH_2 stretch bands in the ir spectrum, as well as their counterparts in the Raman spectrum, are well accounted for by the calculation. (A very weak band is observed at 2868 cm^{-1} in the Raman,⁸ but it is not clear that it is assignable to CH_2 stretch.) The 2980- and 2803-cm^{-1} modes are associated with the $\text{C}^\alpha\text{—H}^\alpha \cdots \text{O}=\text{C}$ bonded CH_2 group, and as can be seen from the potential-energy distribution, they are no longer pure group modes. As a result of the hydrogen bond, the local C_{2v} symmetry of the CH_2 group is lost, and it is therefore not surprising that the stretching modes are not strictly antisymmetric and symmetric combinations of CH stretch.

The amide I frequencies are shifted by transition dipole coupling^{18,19} [for which we used the same parameters as for $(\text{Gly})_n$ I], but not by as much as in the β -sheet.¹⁵ [The calculated uncoupled frequencies (and their shifted values) are: A species— 1649 (1656), 1652 (1651), 1652 (1649); B species— 1650 (1654), 1654 (1653), 1649 (1645).] This is due in part to the fact that although each mode contains contributions from each of the three $\text{C}=\text{O}$ groups, there is partial localization of the vibration and therefore less of an interaction effect. The 1649 (A)- cm^{-1} mode is associated predominantly with the bifurcated $\text{C}=\text{O}$ group, but in the B species both the 1653- and 1645-cm^{-1} modes contain about equal contributions from bifurcated and nonbifurcated groups. As mentioned earlier, since the observed splitting (the strong ir band shows a distinct shoulder at $\sim 1655\text{ cm}^{-1}$)⁴ can essentially

TABLE IV
Observed and Calculated Frequencies (in cm^{-1}) of Antiparallel Chain Crystalline Polyglycine II-ND

Raman	Observed ^a IR	Calculated		Potential Energy Distribution ^b
		A	B	
2980VS	2975W	2980	2980	CH ₂ as(78), CH ₂ ss(18)
2940VS	2940W	{ 2936	{ 2935	CH ₂ as(99)
		2936	2935	
2866VW	2850W	{ 2853	{ 2853	CH ₂ ss(99)
		2853	2853	
2809VW	2408	2803	2803	CH ₂ ss(82), CH ₂ as(22)
		2408	2408	ND s(97)
~2430 ^c		{ 2387	{ 2387	ND s(96)
		2387	2387	
1640VS	1639VS	{ 1649	{ 1651	CO s(72), CN s(22) CO s(74), CN s(22), C ^α CN d(10) CO s(74), CN s(22)
		1647	1645	
		{ 1645	{ 1645	
		1645	1644	
1470M	1476S	1479	1478	C ^α C s(28), CN s(21), CO ib(13), CH ₂ b(12)
		{ 1477	{ 1477	C ^α C s(29), CN s(22), CO ib(13), CH ₂ w(11)
1419S	1420M	1471	1472	C ^α C s(29), CN s(21), CO ib(13), CH ₂ w(10), CO s(10)
		1427	1427	C ^α C s(29), CN s(21), CO ib(13), CH ₂ b(12)
1412W	1350M	1409	1409	C ^α C s(28), CN s(25), CO ib(14), ND ib(12), CH ₂ w(10), CO s(10)
		1404	1404	CH ₂ b(86)
1347W	1333VW	1344	1344	CH ₂ b(83)
		1316	1316	CH ₂ w(69), CH ₂ tw(11)
1267S	1277M	1296	1296	CH ₂ w(77)
		1266	1266	CH ₂ w(79), NC ^α s(18)
1231W	1262M	1252	1252	CH ₂ tw(87)
		1249	1249	CH ₂ tw(87)
1131M	1034M	1128	1128	NC ^α s(61), C ^α C s(13)
		1069	1072	ND ib(43), NC ^α s(24), C ^α C s(14)
		1065	1064	ND ib(38), NC ^α s(29), C ^α C s(14)
			1029	ND ib(46), CH ₂ r(16), C ^α C s(13)

1029M	1028		ND ib(46), CH ₂ r(15), C ^o C s(12)
	1012		NC ^o s(43), ND ib(16)
995VS	1009	987M	NC ^o s(43), ND ib(16), C ^o C s(10)
952W	948		NC ^o s(32), ND ib(22), CH ₂ r(14), C ^o C s(11)
	939		NC ^o s(33), ND ib(22), CH ₂ r(13), C ^o C s(10)
	943		CH ₂ r(50), ND ib(19)
	940		CH ₂ r(57), ND ib(17)
	933		CH ₂ r(50), ND ib(16)
	931		CH ₂ r(44), ND ib(20)
			CH ₂ r(53), ND ib(18)
887W	894	886W	C ^o C s(20), CN s(19), CH ₂ r(16), CO s(12)
875VS	881		CH ₂ r(26), C ^o C s(17), CN s(16)
857W	870		CH ₂ r(19), CN s(19), C ^o C s(18), CO s(11)
734W	740		CH ₂ r(31), C ^o C s(19), CN s(12), NC ^o C d(12)
			CH ₂ r(25), C ^o C s(20), NC ^o C d(14), CN s(13)
			CO ib(23), NC ^o C d(19), CN s(13), CNC ^o d(12)
	702	693S	CO ib(27), NC ^o C d(18)
	700		CO ib(28), NC ^o C d(18)
	592		CO ob(58), CN t(10)
	582		CO ob(59)
576M	576		CO ob(48), CN t(16)
	581		CO ob(46), CO ib(15), ND ob(12)
	576		CO ob(58), CN t(10)
	576		CO ob(55), CO ib(11), ND ob(10)
	531	520S	CN t(58), ND···O ib(25), ND ob(24), CO ob(18)
	505		CN t(24), C ^o CN d(19), ND ob(14), CO ib(11)
			CN t(28), ND ob(19), C ^o CN d(14), CO ib(11), CO ob(11)
491W	495		CN t(42), C ^o CN d(17), ND ob(14)
	475		CN t(38), ND ob(23), C ^o CN d(10)
			CN t(38), C ^o CN d(30), ND ob(18)
			CN t(57), C ^o CN d(22), ND ob(22)

(continued)

TABLE IV (continued)

Observed ^a		Calculated	B	Potential Energy Distribution ^b
Raman	IR			
			462	CN t(48), ND ob(30), C ^o CN d(28), ND t(11)
	356S	457		CN t(62), ND ob(33), C ^o CN d(23), ND t(13)
335W		352	349	NC ^c C d(26), CO ib(17), C ^o CN d(16), CO ob(13)
314VW		344	344	NV ^c C d(27), CO ib(18), C ^o CN d(17), CO ob(14)
		319	318	CO ib(32), CNC ^c d(24), NC ^c C d(17), C ^o CN d(16)
	260M		270	ND ob(23), CO ob(21), NC ^s s(10)
		269		CO ob(22), ND ob(21)
		234		CNC ^o d(59), CO ib(13), D ^o ·O s(12)
			234	CNC ^o d(35), D ^o ·O s(24), C ^o CN d(20)
			225	CNC ^o d(66), CO ib(10)
		218		CNC ^o d(72), CO ib(11)
		191	209	CNC ^o d(55), C ^o CN d(21)
		132		C ^o CN d(44), CNC ^c d(24), NC ^c s(11)
			120	D ^o ·O s(34), CN t(22)
				CN t(30), ND ^o ·O ib(17)
		116	116	CN t(37), ND ob(19), D ^o ·O s(13), ND ^o ·O ib(11)
116W	113S			CN t(35), ND ^o ·O ib(12), ND ob(10), H ^c ··O s(10)
		96		D ^o ·O s(28), ND ob(17), CN t(15), CO t(14), ND t(11), C ^o C t(10)
83W		84	93	ND ob(35), CO t(17), NC ^s t(14), NC ^c C d(13)
			77	ND ob(24), NC ^c C d(16), H ^c ··O s(12), NC ^s t(10)
			74	ND ob(42), ND ^o ·O ib(18), D ^o ·O s(13), CO ^o ·D ib(10), ND ^o ·O ib(10)
		72		ND ob(41), NC ^c C d(15), ND ^o ·O ib(14), C ^o C t(13)
		66		ND ob(44), C ^o C t(18), NC ^c C d(17), ND ^o ·O ib(10)
			62	ND ob(38), ND ^o ·O ib(31), CN t(13), D ^o ·O s(10), ND t(10)
		49		C ^o C t(24), ND ob(17), D ^o ·O s(10)
			43	ND ob(31), D ^o ·O s(12), NC ^c C d(11), C ^o H ^c ··O ib(11), CO t(10)
				ND ob(34), D ^o ·O s(21), ND ^o ·O ib(17), CO ^o ·D ib(11)
		29		ND t(42), CO t(16), CO ^o ·D ib(11), ND ob(11)

^a VS = very strong, S = strong, M = medium, W = weak, VW = very weak.

^b s = stretch, as = antisymmetric stretch, ss = symmetric stretch, b = angle bend, ib = in-plane angle bend, ob = out-of-plane angle bend, w = wag, r = rock, t = torsion, d = deformation, tw = twist. Only contributions of 10% or greater are included. In some cases where contributions to the PEDs of related A and B modes differ by less than 3%, the average value has been given for both frequencies.

^c Unperturbed frequency (see text).

be accounted for by such coupling, we feel justified in assuming the same value of $f(\text{C}=\text{O})$ for all of the peptide groups.

The amide II modes are also shifted by only a small amount as a result of transition dipole coupling, for reasons similar to those for the amide I modes. [The calculated uncoupled frequencies (and their shifted values) are: A species—1567(1565), 1559(1555), 1549(1548); B species—1569(1565), 1557(1552), 1549(1548).] The modes at 1555(A) and 1552(B) cm^{-1} have major, but not sole, contributions from the bifurcated group. The observed splittings are reasonably well reproduced; in fact, the observed structure on the amide II band⁴ may be explained by transition dipole coupling splittings.

The CH_2 bend region shows a definite splitting in the ir spectrum,³ which is well accounted for by our calculation. [A splitting is not seen in the Raman spectrum of $(\text{Gly})_n\text{II}$ but is observed in that of $(\text{Gly})_n\text{II-ND}^8$; as we shall see later, we also predict a larger splitting for the deuterated molecule.] In distinction to the previous simplified calculation,³ our present complete calculation predicts the frequencies of the bonded CH_2 groups at 1433 cm^{-1} . This is more consistent with the intensity distribution in the ir band, as well as the expectation that hydrogen bonding should raise the frequency of the bending mode.

The predominantly CH_2 wag modes, which also contain an NH in-plane bend component, occur in the 1330–1390- cm^{-1} region, the bonded CH_2 groups being predicted to contribute primarily at 1383(A) and 1380(B) cm^{-1} . Two assignable bands are found in the spectra, near 1380 and 1333 cm^{-1} ; these are observed to shift on N-deuteration,^{8,11} confirming the NH contribution to the mode. More significantly, only one band is predicted for the parallel chain structure, thus adding support for the presence of antiparallel chains.

The CH_2 twist mode contributes predominantly in the region of about 1240–1290 cm^{-1} , heavily mixed with CH_2 wag and some NH in-plane bend. Four bands are found that can be assigned to predicted modes, and although they do not select between the two structures, the frequency agreement is better for the antiparallel chain structure.

Skeletal NC^α stretch, with a contribution from C^αC stretch, is found in the region of about 1030–1130 cm^{-1} . The dominant Raman bands at 1031VS and 1134M cm^{-1} are at significantly different frequencies from the essentially similar modes in $(\text{Gly})_n\text{I}$ at 1021VS and 1162M cm^{-1} . The small downward shift in the average frequency and the large decrease in the splitting between these frequencies in $(\text{Gly})_n\text{II}$ as compared to $(\text{Gly})_n\text{I}$ is undoubtedly a result of the conformational difference between these chains, both in terms of geometry as well as its effect on relevant force constants.

Bands in the 860–970- cm^{-1} region are assignable to predicted CH_2 rock modes that are in most cases heavily mixed with skeletal C^αC stretch and CN stretch. The presence of weak Raman bands at 864 and 952 cm^{-1} favors the antiparallel chain structure, since in addition to other common

bands, bands in these regions are predicted by this structure but not by the parallel chain structure.

The observed bands in the region of about 670–750 cm^{-1} arise from modes containing contributions primarily from NH out-of-plane bend, CN torsion, $\text{NH} \cdots \text{O}$ in-plane bend, CO in-plane bend, and NC^αC deformation. The medium-intensity Raman band at 673 cm^{-1} can only be accounted for by the antiparallel chain structure, there being a large gap in predicted frequencies in this region for the parallel chain structure.

A relatively well-defined region between 560 and 590 cm^{-1} is contributed to primarily by CO out-of-plane bend, with some NH out-of-plane bend. Again, it should be noted that the medium-intensity Raman band at 566 cm^{-1} is reasonably accounted for only by the antiparallel chain structure. A narrow region near 500 cm^{-1} is associated with C^αCN deformation. It is interesting to note that in $(\text{Gly})_n\text{I}$, whereas CO out-of-plane bend is found in the range of 590–620 cm^{-1} , C^αCN deformation is divided between modes near 590 and near 290 cm^{-1} .¹⁵ This is undoubtedly due to the conformational differences between the two structures.

The NC^αC deformation coordinate contributes predominantly near 350 cm^{-1} , compared to about 325 cm^{-1} in $(\text{Gly})_n\text{I}$,¹⁵ a result that again probably reflects conformational differences. Mixed NH out-of-plane and CO out-of-plane bend modes near 270 cm^{-1} occur at significantly higher frequencies than in $(\text{Gly})_n\text{I}$, where they are found near 180 cm^{-1} . This may, of course, be a result of the different hydrogen-bond characteristics. The calculated range for CNC^α deformation is only slightly different: about 190–240 cm^{-1} for $(\text{Gly})_n\text{II}$ and 210–250 cm^{-1} for $(\text{Gly})_n\text{I}$.¹⁵

The frequencies containing $\text{H} \cdots \text{O}$ stretch are difficult to assign. In $(\text{Gly})_n\text{I}$ the frequency with the largest contribution [comprising $\text{H} \cdots \text{O}$ stretch (78), CN torsion (18)] is predicted at 111 cm^{-1} and assigned to 112 M cm^{-1} (Raman). In $(\text{Gly})_n\text{II}$ this mode is calculated at 133 cm^{-1} , consistent with our larger value for $f(\text{H} \cdots \text{O})$. No band has been observed at this position, although there is a shoulder in the far-ir spectrum¹³ at ~ 150 cm^{-1} . The observed bands are found near 115 cm^{-1} , and we can at this stage only bracket an appropriate range of calculated bands that contain the expected $\text{H} \cdots \text{O}$ stretch and CN torsion components. It is noteworthy that the 83- cm^{-1} Raman band is of very similar character to the 82- cm^{-1} band of $(\text{Gly})_n\text{I}$, namely, mainly NH out-of-plane bend.

Polyglycine II-ND

The calculated normal modes given in Table IV are for the antiparallel chain structure of $(\text{Gly})_n\text{II-ND}$ since this has been shown to be preferred for $(\text{Gly})_n\text{II}$. The same force constants (Table II) were used in this calculation.

The CH_2 stretch modes follow the pattern for $(\text{Gly})_n\text{II}$. In this case, ir data are not available for all expected bands,¹¹ but the Raman spectra do show four bands.⁸

The assignment of the ND stretch modes is complicated by the lack of detailed information on this region,^{8,11} together with the more complicated Fermi resonance possibilities that occur in deuterated polypeptides.²² Nevertheless, a fairly reasonable analysis of this mode seems possible.

The observed bands at 2472MW and 2419M cm^{-1} in the Raman⁸ and 2464W and 2416S cm^{-1} in the ir¹¹ are clearly assignable to ND stretch in Fermi resonance with a combination band.²² In distinction, however, to $(\text{Gly})_n\text{I-ND}$, the 2416- cm^{-1} band is the stronger of the two, indicating that it should be assigned to ν_A with the 2464- cm^{-1} band being assigned to ν_B , as is the case for $\beta\text{-(L-Ala)}_n\text{-ND}$.²² If we take $I_B/I_A \cong 0.3$ from the Raman⁸ (since no quantitative ir data are available¹¹), neglecting for a moment the existence of two ND stretch modes, then we find²² that $\nu_A^\circ = 2431 \text{ cm}^{-1}$ and $\nu_B^\circ = 2460 \text{ cm}^{-1}$ (these change to 2428 and 2463 cm^{-1} , respectively, for an intensity ratio of 0.2). This value of ν_A° in comparison to that of $(\text{Gly})_n\text{I-ND}$, viz., 2457 cm^{-1} ,¹⁴ shows that it must be associated with the typical N—D ···O=C hydrogen bond in $(\text{Gly})_n\text{II-ND}$, which, as we have seen, is expected to be stronger than that in $(\text{Gly})_n\text{I-ND}$. The value of ν_B° is compatible with combinations comparable to those in other N-deuterated polypeptides,²² namely, $1476 + 995 = 2471$ and $1476 + 987 = 2463$ ($1470 + 995 = 2465$ and $1470 + 987 = 2457$ may also be possible). It is interesting that the ND in-plane bend contribution to the 995- and 987- cm^{-1} bands (see below) is associated entirely with the typical hydrogen bonds, thus justifying the assumption made above. The calculated value of $\nu_A^\circ = 2387 \text{ cm}^{-1}$ is in the range of 40–50 cm^{-1} lower than the observed value, as has been found for other N-deuterated polypeptides²² [being due to the transfer of $f(\text{N—H})$ without compensation for anharmonicity]. The value of $\nu_A^\circ \cong 2430 \text{ cm}^{-1}$ for the typical ND hydrogen bond thus seems quite consistent with expectations, but the question is still left open as to the value of ν_A° for the bifurcated bond. Better experimental data in the ND stretch region will be needed to derive this value, but it is interesting to note that the ir spectrum of $(\text{CD}_2\text{CO})_n\text{II-ND}$ (Ref. 11) shows a more complex structure than does that of $(\text{CH}_2\text{CO})_n\text{II-ND}$: 2485W, 2451W, 2417S. Incidentally, if we use the 40–50- cm^{-1} “rule,” we would expect ν_A° for the bifurcated bond to be in the range of $2408 + (40\text{--}50) = 2448\text{--}2458 \text{ cm}^{-1}$.

The splitting in the amide I region due to transition dipole coupling is predicted to be somewhat less than that in $(\text{Gly})_n\text{II}$. The presently available data^{8,11} do not indicate any splitting, but the region should be reexamined carefully.

Modes in the 1470–1480- cm^{-1} region have the same general character as in $(\text{Gly})_n\text{I-ND}$. No clear single choice, however, is possible at present for the 1476S- cm^{-1} ir band, whereas the higher symmetry of $(\text{Gly})_n\text{I-ND}$ did make this feasible.

The CH_2 bend modes are predicted to shift downward slightly on N-deuteration; this seems to be observed in the Raman spectrum, although the intensity ratio is unexpected (the 1427- cm^{-1} mode is associated with the bonded CH_2 group). The observed large downward shift of the CH_2

wag mode at $\sim 1380\text{ cm}^{-1}$ (to $\sim 1350\text{ cm}^{-1}$) is well predicted, as is the pattern of CH_2 twist modes in the $1230\text{--}1280\text{-cm}^{-1}$ region.

The character of the $\sim 1130\text{-cm}^{-1}$ band is retained from $(\text{Gly})_n\text{II}$ to $(\text{Gly})_n\text{II-ND}$, viz., mainly NC^α with some C^αC stretch, but the nature and frequencies of the modes extending down to $\sim 900\text{ cm}^{-1}$ are altered as a result of the contribution of ND in-plane bend. Thus, although bands remain near 1030 cm^{-1} , they have a very different character. New strong bands are found, and predicted, near 1000 cm^{-1} that contain a significant ND in-plane bend contribution. The frequency decrease of the very strong 884-cm^{-1} Raman band of $(\text{Gly})_n\text{II}$ to 875 cm^{-1} in $(\text{Gly})_n\text{II-ND}$ is very well predicted despite the absence of any ND in-plane bend contribution to this mode.

The bands of $(\text{Gly})_n\text{II}$ in the $670\text{--}750\text{-cm}^{-1}$ region that contain an NH out-of-plane bend contribution of course lose this in the ND compound, and a redistribution of internal coordinates occurs. It is interesting that the 698S-cm^{-1} ir band of $(\text{Gly})_n\text{II}$, which contains no NH out-of-plane bend, retains its character in $(\text{Gly})_n\text{II-ND}$, and, in fact, its slight downward shift is well predicted. Although the main CO out-of-plane bend character of the 573S-cm^{-1} ir band of $(\text{Gly})_n\text{II}$ is retained in the 576M-cm^{-1} Raman band of $(\text{Gly})_n\text{II-ND}$, ND out-of-plane bend begins to contribute to the latter mode and becomes a significant contribution to the 520S-cm^{-1} ir band.

The bands below 500 cm^{-1} follow a pattern similar to that in $(\text{Gly})_n\text{II}$, apparently not being influenced too much by the exchange of NH for ND. The slight decrease of frequencies to 356S cm^{-1} (ir) and 335W cm^{-1} (Raman) is predicted, and the presence of lower-frequency bands is well accounted for. The bands near 115 cm^{-1} are seen to be little affected by the change in contribution from $\text{H}\cdots\text{O}$ stretch to $\text{D}\cdots\text{O}$ stretch.

CONCLUSIONS

Our detailed normal coordinate analysis of the vibrational spectrum of crystalline $(\text{Gly})_n\text{II}$ strongly supports the conclusion that this 3_1 -helical molecule crystallizes in an antiparallel chain structure in which every third residue participates in a $\text{C}^\alpha\text{—H}^\alpha\cdots\text{O}=\text{C}$ hydrogen bond. This derives from the fact that although the backbone forms a 3_1 -helix, strict symmetry is broken by the presence of the above hydrogen bonds, leading to the presence of additional bands in the spectrum. Some of these bands are clearly associated with the characteristically different NH and CH_2 groups present, for example, localized group modes in the NH stretch, CH_2 stretch, and CH_2 bend regions. Others, however, clearly involve combined group and backbone vibrations, such as bands at $\sim 1333\text{ cm}^{-1}$ (primarily CH_2 wag), 952 cm^{-1} (CH_2 rock), and 864 cm^{-1} (primarily CH_2 rock). And still others are associated primarily with backbone modes, as is the case for bands at 673 , 566 , and 340 cm^{-1} . The above bands cannot be accounted for by a parallel chain structure. The presence of extra bands, particularly in the low-frequency region, clearly establishes the loss of strict 3_1 symmetry

and thus implies the existence of $C^\alpha-H^\alpha \cdots O=C$ hydrogen bonds independent of arguments based on additional NH and CH_2 bands.^{3,4} Our results thus provide additional support for the presence of such hydrogen bonds in $(Gly)_n$ II.

The agreement between observed and calculated frequencies is quite good (the average discrepancy between observed and calculated frequencies below 1700 cm^{-1} is about 4.3 cm^{-1}). Force constants involving hydrogen bonds have had to be adjusted from the $(Gly)_n$ I force field, which is not surprising since the hydrogen-bond characteristics are different in these two structures. There are, however, about 70 intramolecular force constants in $(Gly)_n$ I that do not involve hydrogen bonds, and of these, only 10 required adjusting for $(Gly)_n$ II. Studies such as these, as well as those on β -poly(L-alanine)¹⁶ and on α -poly(L-alanine) (data to be published), should provide information on the dependence of the force field on conformation, which it is necessary to know in detail in order to use normal coordinate calculations as a tool in studying the conformations of polypeptide chains.

This research was supported by National Science Foundation grants PCM-7921652 and DMR-7800753.

References

1. Crick, F. H. C. & Rich, A. (1955) *Nature* **176**, 780–781.
2. Ramachandran, G. N., Sasisekharan, V. & Ramakrishnan, C. (1966) *Biochim. Biophys. Acta* **112**, 168–170.
3. Krimm, S., Kuroiwa, K. & Rebane, T. (1966) in *Conformation of Biopolymers*, Ramachandran, G. N., Ed., Academic Press, New York, pp. 439–447.
4. Krimm, S. & Kuroiwa, K. (1968) *Biopolymers* **6**, 401–407.
5. Krimm, S. (1966) *Nature* **212**, 1482–1483.
6. Ramachandran, G. N., Ramakrishnan, C. & Venkatachalam, C. M. (1967) in *Conformation of Biopolymers*, Ramachandran, G. N., Ed., Academic Press, New York, pp. 429–438.
7. Miyazawa, T. (1967) in *Poly- α -Amino Acids*, Fasman, G. D., Ed., Marcel Dekker, New York, pp. 69–103.
8. Small, E. W., Fanconi, B. & Peticolas, W. L. (1970) *J. Chem. Phys.* **52**, 4369–4379.
9. Singh, R. D. & Gupta, V. D. (1971) *Spectrochim. Acta* **27A**, 385–393.
10. Abe, Y. & Krimm, S. (1972) *Biopolymers* **11**, 1841–1853.
11. Suzuki, S., Iwashita, Y., Shimanouchi, T. & Tsuboi, M. (1966) *Biopolymers* **4**, 337–350.
12. Smith, M., Walton, A. G. & Koenig, J. L. (1969) *Biopolymers* **8**, 29–43.
13. Fanconi, B. (1973) *Biopolymers* **12**, 2759–2776.
14. Moore, W. H. & Krimm, S. (1976) *Biopolymers* **15**, 2439–2464.
15. Dwivedi, A. M. & Krimm, S. (1982) *Macromolecules* **15**, 177–185.
16. Dwivedi, A. M. & Krimm, S. (1982) *Macromolecules* **15**, 186–193.
17. Morokuma, K. (1977) *Acc. Chem. Res.* **10**, 294–300.
18. Krimm, S. & Abe, Y. (1972) *Proc. Natl. Acad. Sci. USA* **69**, 2788–2792.
19. Moore, W. H. & Krimm, S. (1975) *Proc. Natl. Acad. Sci. USA* **72**, 4933–4935.
20. Moore, W. H. & Krimm, S. (1976) *Biopolymers* **15**, 2465–2483.
21. Rabolt, J. F., Moore, W. H. & Krimm, S. (1977) *Macromolecules* **10**, 1065–1074.
22. Krimm, S. & Dwivedi, A. M. (1982) *J. Raman Spectrosc.* **12**, 133–137.

Received February 25, 1982

Accepted May 20, 1982